

Ultrafast Charge Transfer Processes Accompanying *KLL* Auger Decay in Aqueous KCl Solution

D. Céolin,¹ N. V. Kryzhevoi,^{2,*} Ch. Nicolas,¹ W. Pokapanich,³ S. Choksakulporn,³ P. Songsiriritthigul,⁴ T. Saisopa,⁴ Y. Rattanachai,⁵ Y. Utsumi,¹ J. Palaudoux,^{6,7} G. Öhrwall,⁸ and J.-P. Rueff^{1,6,7}

¹Synchrotron SOLEIL, l'Orme des Merisiers, Saint-Aubin, F-91192 Gif-sur-Yvette Cedex, France

²Theoretical Chemistry, Institute of Physical Chemistry, Heidelberg University, Im Neuenheimer Feld 229, 69120 Heidelberg, Germany

³Faculty of Science, Nakhon Phanom University, Nakhon Phanom 48000 Thailand

⁴NANOTEC-SUT Center of Excellence on Advanced Functional Nanomaterials and School of Physics,

Suranaree University of Technology, Nakhon Ratchasima 30000, Thailand

⁵Department of Applied Physics, Faculty of Sciences and Liberal Arts, Rajamangala University of Technology Isan, Nakhon Ratchasima 30000, Thailand

⁶CNRS, UMR 7614, Laboratoire de Chimie Physique-Matière et Rayonnement, F-75005 Paris, France

⁷Sorbonne Universités, UPMC Université Paris 06, UMR 7614, Laboratoire de Chimie Physique-Matière et Rayonnement, F-75005 Paris, France

⁸MAX IV Laboratory, Lund University, P.O. Box 118, SE-22100 Lund, Sweden

(Received 16 June 2017; published 29 December 2017)

X-ray photoelectron and *KLL* Auger spectra were measured for the K^+ and Cl^- ions in aqueous KCl solution. While the XPS spectra of these ions have similar structures, both exhibiting only weak satellites near the main line, the Auger spectra differ dramatically. Contrary to the chloride case, a very strong extra peak was found in the Auger spectrum of K^+ at the low kinetic energy side of the 1D state. Using the equivalent core model and *ab initio* calculations this spectral feature was assigned to electron transfer processes from solvent water molecules to the solvated cation. The observed charge transfer processes are suggested to play an important role in charge redistribution following single and multiple core-hole creation in atoms and molecules placed into environment.

DOI: 10.1103/PhysRevLett.119.263003

Charge transfer (CT) processes are of wide relevance in chemistry, physics, and biology. They are reportedly responsible for important transformations in living organisms and are involved in fundamental steps describing, e.g., the photosynthesis [1] and respiration [2] mechanisms. Electron and charge transport can be exploited for damage recognition and repair in DNA [3,4]. Naturally, the use of such very fast elemental processes for technological purposes has attracted an extraordinary large scientific interest—both theoretically and experimentally—for instance, on energy conversion in photovoltaic or optoelectronic devices (see, e.g., Ref. [5]).

CT processes may accompany core-hole creation in atoms and molecules surrounded by ligands. X-ray photoemission spectroscopy (XPS) turns out to be a powerful probe of CT processes which show up as well-defined low-energy satellites in the XPS spectra. Particularly strong CT satellites were found in XPS spectra of weak chemisorption systems [6,7], in crystals [8,9], and in weakly bound atomic [10] and microsolvated [11–14] clusters. As shown in the latter studies, the energies and intensities of the CT satellites are sensitive to cluster geometries. Furthermore, the type of solvent molecules and their number have strong effects on the CT states [15].

For elements from the first rows of the periodic table, electronic Auger decay is the main relaxation channel of

core-hole states. The lifetimes of these states usually range in the femtosecond and subfemtosecond time scales and may serve as internal reference clocks. Using these references, the core-hole clock method allows one to determine time scales of various processes competing to Auger decay, including ultrafast CT processes induced by inner-shell ionization [4,16,17]. For purely resonant core-excited states, the use of a photon bandwidth narrower than the core-hole lifetime broadening allows a control over possible fast dynamical processes as demonstrated in Ref. [18].

Recently, the core-hole clock method was applied for determination of the intermolecular Coulombic decay (ICD) time scale in core-ionized aqueous solutions [19]. Contrary to Auger decay, ICD is a nonlocal electronic decay process involving environment of the ionized species. Originally, it was predicted for inner-valence-ionized weakly bound systems [20], but can also operate after core ionization and efficiently compete with local Auger decay [21]. Another nonlocal electronic decay process is the electron transfer mediated decay (ETMD) [22], which was also observed in aqueous solution [23]. As processes leading to charge redistribution, nonlocal electronic decays are believed to play an important role in nanoplasma formation in clusters irradiated by intense hard x-ray free-electron-laser (XFEL) pulses [24,25].

In this Letter, we address yet another mechanism of charge redistribution induced by core ionization. Here, the created core-hole state of the solute, typically $1s^{-1}$, undergoes *KLL* Auger decay in which two deep $2p$ core vacancies are produced. Compared to the initial core ionization, a sudden creation of two core holes in the *KLL* Auger decay induces even larger perturbation in the valence region and, thus, strong shake-up excitations. Some of these excitations have CT character. Strong CT satellites were already detected in *KLL* Auger spectra of solid state samples [26]. In the present study, we observe them for the first time in a weakly bound system, namely, in KCl aqueous solution. The corresponding CT processes occur from solvent water molecules, which get ionized by donating their electrons to the solute ion experiencing charge reduction instead. Note that in the absence of ICD and ETMD (water molecules have no $2p$ core electrons) the above CT processes represent the only efficient mechanism of charge redistribution in the *KLL* electronic decay step. Being very fast in the femtosecond and subfemtosecond time scales, they compete with the charge buildup caused by Auger decay.

The experiment was performed on the newly operational setup dedicated to measurements of liquids and specifically designed for the HAXPES station [27] of the GALAXIES beam line [28] of the SOLEIL synchrotron facility, France (details of this setup will be given elsewhere). It is based on the design presented in Ref. [29]. In short, the injection chain is composed of a HPLC pump and a $30\ \mu\text{m}$ glass capillary facing a catcher used to extract the liquid from the vacuum chamber, both placed in a differentially pumped tube. The liquid jet is set perpendicular to the photon beam propagation axis and to the spectrometer lens axis. We performed measurements on $0.5M$ and $1M$ KCl aqueous solutions that were prepared by mixing $>99\%$ KCl salt with deionized water. Filtering and degassing procedures were systematically performed on the solutions. The spectrometer resolution of about $0.6\ \text{eV}$ was achieved with the $500\ \text{eV}$ pass energy and $0.5\ \text{mm}$ slits. The photon energy resolution achieved at $5\ \text{keV}$ was about $0.6\ \text{eV}$.

The $1s$ XPS spectra of the aqueous Cl^- and K^+ ions were recorded at $h\nu = 5\ \text{keV}$ far enough from the $1s$ ionization thresholds to avoid postcollision interaction effects (Fig. 1). The incident energy was calibrated using the $\text{O}1s$ peak position in liquid water ($538.1\ \text{eV}$ [30]). The $1s$ ionization potentials (IPs) of Cl^- and K^+ were found at 2825.4 and $3611.9\ \text{eV}$, respectively. The Lorentzian contributions extracted from the main lines have the full width at half-maximum of $0.62\ \text{eV}$ for aqueous Cl^- and $0.72\ \text{eV}$ for aqueous K^+ , and compare well with the theoretical values obtained for atomic chlorine ($0.64\ \text{eV}$) and potassium ($0.74\ \text{eV}$) [31]. These values correspond to the core-hole lifetimes of 0.9 and $1\ \text{fs}$, respectively. As seen from Fig. 1, apart from the main line each XPS spectrum exhibits a broad satellite region extended towards low kinetic energy and separated from the main line by about $6\text{--}7\ \text{eV}$.

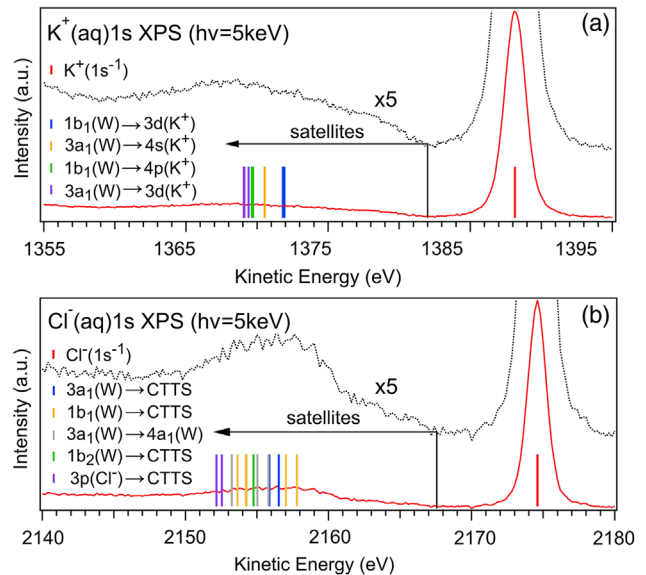


FIG. 1. The $1s$ XPS spectra of K^+ (a) and Cl^- (b) in aqueous KCl solution recorded at photon energy $h\nu = 5\ \text{keV}$ (red lines). A $5\times$ zoom (black line) in each spectrum highlights the presence of a satellite structure at the low kinetic (high binding) energy side of the main line. The bars indicate the energies of the computed main states and low-energy satellites in monohydrated clusters. All satellites in the calculated spectrum of $\text{K}^+(\text{H}_2\text{O})$ [panel (a)] have the CT character and are attributed to electron transfer from water (W) to K^+ . The spectrum of $\text{Cl}^-(\text{H}_2\text{O})$ [panel (b)] is more complex and contains excitations from water and Cl^- to charge-transfer-to-solvent (CTTS, see text) states. Electronic excitations occurring entirely within the water molecule are also present here.

The $1s$ core-ionized K^+ and Cl^- ions are unstable and relax mostly via Auger decay processes. The $\text{KL}_{2,3}\text{L}_{2,3}$ Auger decay produces $2p^{-2}$ double core-hole states represented by the 1S , 1D , and 3P terms, wherein the Auger transitions giving rise to the 3P term are forbidden from parity-conservation rules (cf. Fig. 2). Information on the energy positions of these lines for chlorine and potassium containing molecules is rather scarce, and to the best of our knowledge is not available in the literature for solvated ions.

Cleff and Mehlhorn measured the *KLL* Auger spectrum of Cl in CCl_4 and found the 1D line at the kinetic energy of $2382.8 \pm 1\ \text{eV}$ [32]. This experimental result agrees well with earlier theoretical results predicting the kinetic energies of the 1S , 1D , and 3P lines at 2370 , 2382 , and $2391\ \text{eV}$, respectively [33]. Vayrynen *et al.* [34] measured the *KLL* Auger spectrum of chlorine in HCl and determined the positions of the 1S and 3P lines at -8.5 and $6.4\ \text{eV}$, respectively, relative to the energy of the 1D line at $2372.3\ \text{eV}$. The *KLL* Auger spectrum of aqueous Cl^- [Fig. 2(b)] agrees well with these spectra: We found two strong peaks at the kinetic energies of 2372 and $2381\ \text{eV}$ which are attributed to the 1S and 1D states, respectively, and a weaker structure at $\sim 2388.5\ \text{eV}$, assigned to the 3P state.

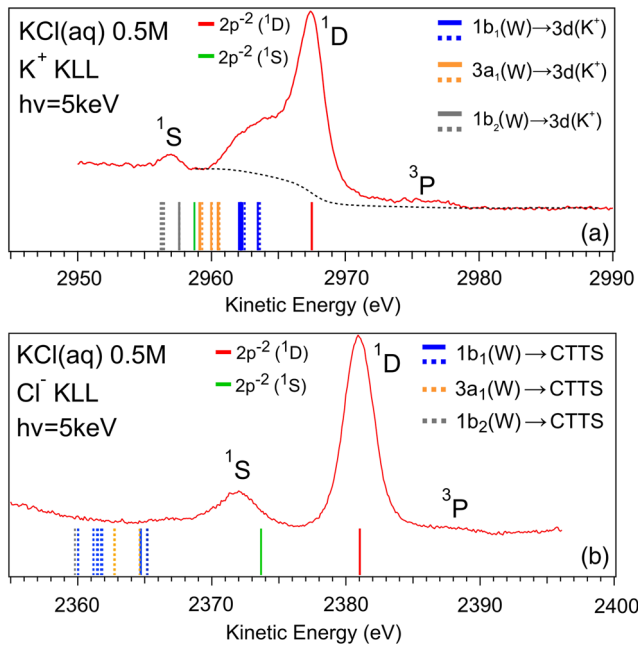


FIG. 2. The *KLL* Auger spectra of K^+ (a) and Cl^- (b) in aqueous KCl solution recorded at photon energy $h\nu = 5$ keV. In the spectrum of potassium, a Shirley background is shown by a black dotted curve. The bars indicate the energies of the calculated $2p^{-2}$ double core-hole main 1D and 1S states and satellites in monohydrated clusters. The satellites are mostly associated with the 1D state and can be either singlets (solid lines) or triplets (dashed lines). The calculated main 3P states and corresponding satellites are not shown due to their weak intensities. All low-energy satellites in the theoretical spectra are CT states attributed to electron transfer processes from water (*W*) to either K^+ (panel a) or to the CTTS states (panel b).

For potassium, the literature is even poorer. Lohmann and Fritzsche [35] calculated the *KLL* Auger spectrum of atomic potassium and obtained the kinetic energy of 2959.82 eV for the $2p^4(^1D)4s$ state, 2950.49 eV for the $2p^4(^1S)4s$ state, and an energy window ranging from 2966.73 to 2969.62 eV for the $2p^4(^3P)4s$ state. The *KLL* Auger spectrum of aqueous K^+ has a remarkably different shape (Fig. 2). It has two peaks at 2957 and 2967.4 eV kinetic energy, and a weaker structure around ~ 2976.3 eV, which are assigned to the 1S , 1D , and 3P states, respectively. In addition, a very intense extra peak is observed at the low kinetic energy side of the 1D state, at ~ 2963 eV, which is not present in the Auger spectrum of aqueous chloride. We note that neither the change in salt concentration from 0.5M to 1M, nor the decrease of the photon flux by a factor of 10 led to noticeable modifications in the shape of the potassium spectrum.

Before we explain this extra feature, let us focus first on the satellite regions in the XPS spectra of both aqueous ions. According to our calculations the first satellite in the XPS spectrum of atomic K^+ is separated from the main line

by about 40 eV. Thus, the low-energy satellites in the spectrum of solvated K^+ do not correspond to local excitations but rather found their origin in the presence and involvement of solvent water molecules. To gain more insight we computed the energies of several core-ionized states in microsolvated $K^+(H_2O)$ and $K^+(H_2O)_2$ clusters (similar calculations were carried out also for the atomic Cl^- anion and a $Cl^-(H_2O)$ cluster). The computations of the $1s^{-1}$ single- and $2p^{-2}$ double-core-hole states of microsolvated and atomic ions were performed using the occupation-restricted-multiple-active-space single- and double-excitation configuration interaction method as implemented in the GAMESS(US) package [36]. All core orbitals except for the considered ones were kept frozen. We used the 6-311 + G^* basis set for potassium and chlorine, and the 6-311G* one for oxygen and hydrogen atoms [37]. The cluster geometries were taken from Refs. [11,19].

The results for the monohydrated $K^+(H_2O)$ cluster are shown in Fig. 1(a) as bars (an energy shift of 1.87 eV was applied to adjust the main lines in the experimental and theoretical spectra). All low-energy satellites in the theoretical spectrum have a CT character and correspond to excitations of valence electrons from the water molecule to vacant orbitals of the potassium cation. The first satellites are separated from the main line by about 16 eV and are attributed to excitations of a water's $1b_1$ electron to the unoccupied $3d$ orbital of potassium, $1b_1(H_2O) \rightarrow 3d(K^+)$. These satellites are followed by the $3a_1(H_2O) \rightarrow 4s(K^+)$ and $1b_1(H_2O) \rightarrow 4p(K^+)$ CT states. In the dihydrated cluster, the energy separation between the main line and the first satellites increases to 20.5 eV (not shown). The same trend with cluster size was found also in the XPS spectra of microsolvated Na^+ [15]. The CT states in the theoretical spectra have thus nearly the same energies as the intensity maximum of the experimental satellite feature at ~ 1368 eV. This is a strong indication that, at least partially, this feature has a CT contribution. Note that the first satellites in the experimental spectrum appear already at 6 eV from the main line, where theory predicts no states. We attribute them to energy losses of emitted photoelectrons due to inelastic scattering from water. The onset of these satellites matches the band gap of 6.9 eV in liquid water quite well (see Ref. [38] and references therein). The energy-loss states spread then to lower kinetic energies and overlap with the CT satellites.

In the computed XPS spectrum of atomic Cl^- the lowest-energy satellites, corresponding to the $3p(Cl^-) \rightarrow 4p(Cl^-)$ excitations, are separated from the main line by 19 eV. In the $Cl^-(H_2O)$ cluster, the unoccupied $4p$ and $4s$ orbitals of Cl^- are mixed with each other and also with empty orbitals of the water molecule. We call these resulted hybrid orbitals the precursory charge-transfer-to-solvent (CTTS) states as they resemble the CTTS states in aqueous anions, namely, they are related to the anion, diffuse and have asymmetric

shapes occupying predominantly the solvent-free space [39,40]. The computed XPS spectrum of $\text{Cl}^-(\text{H}_2\text{O})$ [Fig. 1(b)] exhibits excitations to these CTTS orbitals from chloride and water. The latter transitions are more numerous and lie closer to the main line. As seen from Fig. 1(b), the excitations to the CTTS states fit well with the position of the experimental satellite structure centered at 2157 eV. The experimental spectrum should also contain energy-loss states and the first such states likely form the satellites' onset at 7 eV above the main line. Analogous states, e.g., $3a_1(\text{H}_2\text{O}) \rightarrow 4a_1(\text{H}_2\text{O})$, are found also in the theoretical spectrum although at rather high energies as a consequence of small cluster size.

Since all satellites in the XPS spectrum of aqueous K^+ are very weak (their total intensity is about 14 times smaller than the intensity of the main line), Auger decay of these states cannot contribute significantly to the K^+ *KLL* Auger spectrum. The appearance of the strong extra peak at 2963 eV in the latter spectrum with the intensity of only about 3 times weaker than the 1D line (after subtraction of the Shirley background shown in Fig. 2(a) by the black dotted curve) cannot be explained by these relaxation processes alone. The high intensity of this peak and its close proximity to the 1D main line also do not suggest that this peak appears entirely due to inelastic scattering processes of Auger electrons. Apparently, this spectral feature has a different origin.

A similar structure was found earlier in the *KLL* Auger spectra of various solid potassium compounds and assigned to electron transfer processes from ligands to core-ionized potassium [26]. Since counterions are far separated from each other in the low-concentrated KCl aqueous solutions studied here (0.5M and 1M), chloride anions can hardly be involved in the CT processes. On the contrary, solvent water molecules are able to donate their electrons to neighboring core-ionized K^+ cations and their separations from these cations are rather short (2.65 Å [41]).

Assuming that water molecules are involved in the CT processes, we express the difference between the energy of the main line, E_{ML} , and the energy of a CT satellite, E_{CT} , in the K^+ *KLL* Auger spectrum as follows:

$$\Delta E = E_{\text{CT}} - E_{\text{ML}} = E(\text{K}_{cc}^{2+} \text{H}_2\text{O}^+) - E(\text{K}_{cc}^{3+} \text{H}_2\text{O}) + \text{RE}, \quad (1)$$

where c denotes a $2p$ core hole, and RE is the Coulomb repulsion energy between the potassium dication and a water cation. Using the $Z + 2$ equivalent core model, we substitute the core-ionized potassium by its equivalent-core ion, Sc, and get

$$\begin{aligned} \Delta E = E_{\text{CT}} - E_{\text{ML}} &= E(\text{Sc}^{2+} \text{H}_2\text{O}^+) - E(\text{Sc}^{3+} \text{H}_2\text{O}) + \text{RE} \\ &= -\text{IP}(\text{Sc}^{2+}) + \text{IP}(\text{H}_2\text{O}) + \text{RE}, \quad (2) \end{aligned}$$

where IP refers to the outer-valence ionization potential in solution. Contrary to the well-known IPs of liquid water, those of aqueous Sc^{2+} are not available since this dication does not exist in aqueous solutions. We shall use a value of 8.76 eV obtained by subtracting the solvation shift of aqueous Ca^{2+} (~16 eV [42]) from the IP of gas-phase Sc^{2+} (24.76 eV [43]). By substituting this value and the lowest IP of liquid water (11.16 eV [44]) into Eq. (2) and neglecting for the moment the repulsion energy RE (the Coulomb interaction is largely screened in solutions [21,45]), we obtain ΔE of 2.4 eV which agrees rather well with the experimental observation of 4.4 eV.

This is, however, a crude estimate. In order to gain more insight into the CT processes accompanying the K^+ *KLL* Auger decay we computed the energies of the final Auger states in the $\text{K}^+(\text{H}_2\text{O})$ and $\text{K}^+(\text{H}_2\text{O})_2$ clusters. The main 1D and 1S states together with the associated low-lying satellites in the monohydrated cluster are shown in Fig. 2(a) as bars (the satellites can be either singlets (solid lines) or triplets (dashed lines) according to the multiplicity of the single excitation on top of the double core vacancy). We shifted them to adjust the energies of the 1D lines in the experimental and theoretical spectra. The main 3P state and all related satellites are not plotted because of their small intensities.

The first satellites in the theoretical Auger spectrum lie about 4 eV away from the 1D state, in agreement with the position of the strong experimental satellite peak. These states correspond to electron transfer from the water's outermost $1b_1$ orbital to the unoccupied $3d$ orbital of potassium, $1b_1(\text{H}_2\text{O}) \rightarrow 3d(\text{K}^+)$ in the presence of the $2p^{-2}$ (1D) double core hole on potassium. The CT satellites $3a_1(\text{H}_2\text{O}) \rightarrow 3d(\text{K}^+)$ and $1b_2(\text{H}_2\text{O}) \rightarrow 3d(\text{K}^+)$ appear at higher kinetic energies overlapping with the 1S main state. The electronic transitions from water to the $4s$ and $4p$ orbitals of potassium are even more energetic and the respective satellites are found at the lower kinetic energy side of the 1S state (not shown), where the experimental spectrum show no satellite peaks.

Note that neither the *LMM* Auger spectra of aqueous K^+ and Ca^{2+} [19,45] nor the *KLL* Auger spectrum of solvated Na^+ [42] exhibit any intense satellites. This is because the corresponding Auger processes create outer-valence double vacancies and do not induce strong electron relaxation as in the case of the double core-hole creation in the K^+ *KLL* Auger decay. Surprisingly, although the Cl^- *KLL* Auger decay also produces a double core hole, no obvious low-lying satellites were found in the respective spectrum [Fig. 2(b)]. This may have several reasons. One of them is the large anion-water distances (3.16 vs 2.65 Å in aqueous K^+ [41]) making the CT processes in aqueous Cl^- less efficient than in aqueous K^+ . Furthermore, the Coulomb attraction between the created double core-hole and the electrons of neighboring molecules is reduced due to a screening effect of the excess electron of Cl^- . According to our calculations, the Auger spectrum of

$\text{Cl}^-(\text{H}_2\text{O})$ does have satellites but they are more separated (16 eV and more) from the main 1D line than in $\text{K}^+(\text{H}_2\text{O})$ (Fig. 2). The absence of low-lying vacant orbitals in chloride explains this behavior. The first such satellites correspond to the electronic transitions from water to the CTTS states. Probably, the very weak feature at 2367 eV in the experimental spectrum originates from these transitions. The excitations of the $3p(\text{Cl}^-)$ electrons to the CTTS states were not found among the low-energy satellites. These have higher energies and might be responsible of the spectral structure starting at about 2355 eV.

To summarize, we performed the first high kinetic energy photoemission experiments on an aqueous salt solution. By measuring XPS and *KLL* Auger spectra we highlighted CT processes from solvent water molecules to solvated ions which were not observed in aqueous media before. These CT processes accompany the single and double core-hole creations, occur with the latter on the same time scales (the core-hole lifetimes) and, thus, are ultrafast. The particularly high intensity of the CT satellite peak in the K^+ *KLL* Auger spectrum suggests a high efficiency of the corresponding CT processes. This efficiency depends on many factors, especially on the ionic charge, ion-water distances, and the electronic shell where the single and double core holes are created inducing large relaxation effects.

The occurrence of CT processes in aqueous environments may have implications for radiation therapy. Until now the therapeutic effect of K-shell-ionized Auger electron emitters was entirely ascribed to energetic Auger electrons affecting biomolecules both directly and indirectly [46]. Our study demonstrates that *KLL* Auger decay also efficiently produces harmful water radical cations, and the effectiveness of such Auger processes is actually higher than it was thought before.

The above CT processes deserve special attention also because of the occurring ultrafast charge redistribution and ensuing structural changes in x-ray irradiated objects. The time scale of these changes is relevant, e.g., for XFEL-based experiments on object imaging.

An open question remains whether the addressed CT processes may also occur in rare-gas clusters characterized by rather large interatomic distances. The possible contribution of these processes into x-ray-induced charge redistribution and nanoplasma formation [24,25] should be carefully examined in future studies.

Experiments were performed at the GALAXIES beam line, SOLEIL Synchrotron, France (Proposal No. 20140160). The authors are grateful to the SOLEIL staff for assistance during the beam time and to P. Morin for supporting this project. N. V. K. thanks the Deutsche Forschungsgemeinschaft for financial support and Dr. V. Stumpf for help with calculations. We are grateful to Dr. M. Tashiro for valuable discussions. Campus France and the PHC SIAM exchange program are acknowledged for financial support.

*Corresponding author.

nikolai.kryzhevoi@pci.uni-heidelberg.de

- [1] S. Eberhard, G. Finazzi, and F. A. Wollmann, *Annu. Rev. Genet.* **42**, 463 (2008).
- [2] M. Cordes and B. Giese, *Chem. Soc. Rev.* **38**, 892 (2009).
- [3] H. Ikeura-Sekiguchi and T. Sekiguchi, *Phys. Rev. Lett.* **99**, 228102 (2007).
- [4] S. R. Rajsiki, B. A. Jackson, and J. K. Barton, *Mutat. Res.* **447**, 49 (2000).
- [5] M. A. Loi and A. Troisi, *Phys. Chem. Chem. Phys.* **16**, 20277 (2014).
- [6] A. Nilsson, H. Tillborg, and N. Mårtensson, *Phys. Rev. Lett.* **67**, 1015 (1991).
- [7] N. V. Dobrodey, L. S. Cederbaum, and F. Tarantelli, *Surf. Sci.* **402–404**, 508 (1998).
- [8] R. P. Vasquez, C. U. Jung, M.-S. Park, H.-J. Kim, J. Y. Kim, and S.-I. Lee, *Phys. Rev. B* **64**, 052510 (2001).
- [9] N. V. Dobrodey, A. I. Streltsov, L. S. Cederbaum, C. Villani, and F. Tarantelli, *Phys. Rev. B* **66**, 165103 (2002).
- [10] N. V. Dobrodey, A. I. Streltsov, and L. S. Cederbaum, *Phys. Rev. A* **65**, 023203 (2002).
- [11] A. I. Streltsov, N. V. Dobrodey, and L. S. Cederbaum, *J. Chem. Phys.* **119**, 3051 (2003).
- [12] N. V. Kryzhevoi, N. V. Dobrodey, and L. S. Cederbaum, *J. Chem. Phys.* **122**, 104304 (2005).
- [13] N. V. Kryzhevoi and L. S. Cederbaum, *J. Chem. Phys.* **123**, 154308 (2005).
- [14] N. V. Kryzhevoi, F. Tarantelli, and L. S. Cederbaum, *Chem. Phys. Lett.* **626**, 85 (2015).
- [15] N. V. Kryzhevoi and L. S. Cederbaum, *J. Chem. Phys.* **130**, 084302 (2009).
- [16] O. Björneholm, A. Nilsson, A. Sandell, B. Hernäs, and N. Mårtensson, *Phys. Rev. Lett.* **68**, 1892 (1992).
- [17] A. Föhlisch, P. Feulner, F. Hennies, A. Fink, D. Menzel, D. Sanchez-Portal, P. M. Echenique, and W. Wurth, *Nature (London)* **436**, 373 (2005).
- [18] F. Gel'mukhanov and H. Ågren, *Phys. Rev. A* **54**, 3960 (1996).
- [19] W. Pokapanich, N. V. Kryzhevoi, N. Ottosson, S. Svensson, L. S. Cederbaum, G. Öhrwall, and O. Björneholm, *J. Am. Chem. Soc.* **133**, 13430 (2011).
- [20] L. S. Cederbaum, J. Zobeley, and F. Tarantelli, *Phys. Rev. Lett.* **79**, 4778 (1997).
- [21] P. Slavíček, B. Winter, L. S. Cederbaum, and N. V. Kryzhevoi, *J. Am. Chem. Soc.* **136**, 18170 (2014).
- [22] J. Zobeley, R. Santra, and L. S. Cederbaum, *J. Chem. Phys.* **115**, 5076 (2001).
- [23] I. Unger, R. Seidel, S. Thürmer, M. N. Pohl, E. F. Aziz, L. S. Cederbaum, E. Muchová, P. Slavíček, B. Winter, and N. V. Kryzhevoi, *Nature Chem.* **9**, 708 (2017).
- [24] T. Tachibana *et al.*, *Sci. Rep.* **5**, 10977 (2015).
- [25] K. Ueda (private communication).
- [26] S. Nishikida and S. Ikeda, *J. Electron Spectrosc. Relat. Phenom.* **13**, 49 (1978).
- [27] D. Céolin, J. M. Ablett, D. Prieur, T. Moreno, J. P. Rueff, T. Marchenko, L. Journel, R. Guillemin, B. Pilette, T. Marin, and M. Simon, *J. Electron Spectrosc. Relat. Phenom.* **190**, 188 (2013).
- [28] J. P. Rueff, J. M. Ablett, D. Céolin, D. Prieur, T. Moreno, V. Balédent, B. Lassalle-Kaiser, J. E. Rault, M. Simon, and A. Shukla, *J. Synchrotron Radiat.* **22**, 175 (2015).

- [29] M. Faubel, S. Schlemmer, and J. P. Toennies, *Z. Phys. D* **10**, 269 (1988).
- [30] B. Winter and M. Faubel, *Chem. Rev.* **106**, 1176 (2006).
- [31] M. O. Krause and J. H. Oliver *J. Phys. Chem. Ref. Data* **8**, 329 (1979).
- [32] B. Cleff and W. Mehlhorn, *Z. Phys.* **219**, 311 (1969).
- [33] K. Siegbahn, C. Nordling, A. Fahlman, R. Nordberg, K. Hamrin, J. Hedman, G. Johansson, T. Bergmark, S.-E. Karlsson, I. Lindgren, and B. J. Lindberg, *ESCA: Atomic, Molecular, and Solid State Structure Studies by Means of Electron Spectroscopy*, Nova Acta Regiae Societatis Scientiarum Upsaliensis Series IV, Vol. 20 (Upsala, 1967).
- [34] J. Vayrynen, R. N. Sodhi, and R. G. Cavell, *J. Chem. Phys.* **79**, 5329 (1983).
- [35] B. Lohmann and S. Fritzsche, *J. Phys. B* **27**, 2919 (1994).
- [36] M. W. Schmidt, K. K. Baldrige, J. A. Boatz, S. T. Elbert, M. S. Gordon, J. H. Jensen, S. Koseki, N. Matsunaga, K. A. Nguyen, S. J. Su, T. L. Windus, M. Dupuis, and J. A. Montgomery, *J. Comput. Chem.* **14**, 1347 (1993).
- [37] J.-P. Blaudeau, M. P. McGrath, L. A. Curtiss, and L. Radom, *J. Chem. Phys.* **107**, 5016 (1997).
- [38] C. Fang, W.-F. Li, R. S. Koster, J. Klimes, A. Van Blaaderen, and M. A. Van Huis, *Phys. Chem. Chem. Phys.* **17**, 365 (2015).
- [39] M. J. Blandamer and M. F. Fox, *Chem. Rev.* **70**, 59 (1970).
- [40] S. E. Bradforth and P. Jungwirth, *J. Phys. Chem. A* **106**, 1286 (2002).
- [41] Y. Marcus, *Chem. Rev.* **109**, 1346 (2009).
- [42] H. Siegbahn, M. Lundholm, S. Holmberg, and M. Arbman, *Phys. Scr.* **27**, 431 (1983).
- [43] C. H. H. Van Deurzen, J. G. Conway, and S. P. Davis, *J. Opt. Soc. Am.* **63**, 158 (1973).
- [44] B. Winter, R. Weber, W. Widdra, M. Dittmar, M. Faubel, and I. V. Hertel, *J. Phys. Chem. A* **108**, 2625 (2004).
- [45] W. Pokapanich, H. Bergersen, I. L. Bradeanu, R. R. T. Marinho, A. Lindblad, S. Legendre, A. Rosso, S. Svensson, O. Björneholm, M. Tchapyguine, G. Öhrwall, N. V. Kryzhevoi, and L. S. Cederbaum, *J. Am. Chem. Soc.* **131**, 7264 (2009).
- [46] R. W. Howel, *Int. J. Radiat. Biol.* **84**, 959 (2008).